Electronic Supplementary Material (ESI) for Journal of Materials Chemistry A.

Electronic Supplementary Information

Ball-milling Synthesis of Co_2P Nanoparticles Encapsulated Nitrogen Doped Hollow Carbon Rods as Efficient Electrocatalysts

Haitao Wang,[a] Wei Wang,[a] Yang Yang Xu,[a] Muhammad Asif,[a] Hongfang Liu,*[a] and Bao Yu Xia ,*[a,b]

[a] *Key laboratory of Material Chemistry for Energy Conversion and Storage (Ministry of Education), Hubei Key Laboratory of Material Chemistry and Service Failure, School of Chemistry and Chemical Engineering, Wuhan National Laboratory for Optoelectronics, Huazhong University of Science and Technology (HUST), 1037 Luoyu Road, Wuhan 430074, P. R. China*

[b] *Shenzhen Institute of Huazhong University of Science and Technology, Shenzhen 518000, P. R. China*

* Corresponding Author. E-mail: byxia@hust.edu.cn (B. Y. Xia); liuhf@hust.edu.cn (H. Liu).

Experimental section

Synthesis of Co_2P/N-HCR

Typically, different amounts (45, 30 and 15 mmol) of citric acid ($C_6H_8O_7$•H_2O), 2.5 mmol of diammonium phosphate ($(NH_4)_2HPO_4$) and 5 mmol of cobalt acetate ($Co(CH_3COO)_2$•$4H_2O$) are placed into a vacuum stainless steel container. Subsequently, the capsule is sealed and agitated at 500 rpm by ball-milling in a planetary ball-mill equipment (QM-3SP04) for 10 h. The resulting product is extracted with ethanol, then dried up at 60 °C to obtain precursor. Finally, the precursor is annealed at 350 °C under flowing high purity N_2 for 1 h, then at 750 °C for another 3 h. Afterward, the final products are collected after cooling down, and are designated as Co_2P/N-HCR-1, Co_2P/N-HCR-2 and Co_2P/N-HCR-3, respectively, which are dependent on the different moles of citric acid (45, 30 and 15 mmol). For comparison, the samples obtained at the different atomic ratio for P and Co (1:1, 1:2 and 1:3) are synthesized by a similar method (maintain the content of citric acid in 30 mmol and the total content of P and Co in 7.5 mmol). The N-free control sample is prepared in a similar way just replace $(NH_4)_2HPO_4$ with Na_2HPO_4 in the process of synthesis, and the distilled water washing is the necessary to remove the sodium ions. Additionally, to elucidate the role of the unique hollow rod structure, the final Co_2P/N-HCR sample is ground by high-energy ball milling, which can destroy the tubular structure. Furthermore, high-energy ball milling control catalyst is also subjected to etching of hot 0.5 M H_2SO_4 aqueous to study the importance of the encapsulated Co_2P nanoparticles.

Characterization

The surface morphology and composition is tested by FE-SEM (Nova NanoSEM 450) and an energy-dispersive X-ray spectroscope (EDX). The microstructure is studied by HRTEM (Tecnai G2 F20 S-TWIN). The crystalline structures is characterized by XRD (Bruker AXS D2 diffractometer). Raman spectroscopy for is taken with a confocal Raman microscope (LabRAM HR800). The surface area (BET) and pore size distributions (PSD) of all catalysts are recorded by N_2 adsorption-desorption isotherm on a surface analyzer (ASAP 2020, Micromeritics USA). The electronic structures and surface chemical components of all catalysts are analyzed by XPS (AXIS-ULTRA DLD-600W).

Electrochemical measurements

The samples are evaluated electrochemically using an Autolab CHI760E potentiostat/galvanostat with the Pine research instrumentation (AFCBP1 biopotentiostat and AFMSRX rotator) in standard three-electrode electrochemical cell at 25 °C, in which a catalyst-coated glassy carbon electrode (GCE, 5 mm in diameter), a platinum plate and 0.1 M KOH are used as the working electrode, counter electrode and electrolyte, respectively. The saturated calomel electrode (SCE) reference electrode is calibrated using reversible hydrogen electrode (RHE). All the potential values used in this study are given relative to the RHE scale. To fabricate the catalysts ink, 5 mg of catalysts powder and 20 μL of Nafion solution (5 wt %) are ultrasonically dispersed in 0.98 mL of isopropyl alcohol for 30 min. Subsequently, 14 μL of the testing catalysts are pipetted onto the surface of GCE corresponding a catalyst amount of 0.357 mg cm^{-2}. For comparison, a Pt loading (20% Pt/C, ETEK) of 20 μg cm^{-2} is employed in our work.

In the ORR measurements, O_2 and N_2 are applied to obtain O_2-rich and O_2-free environments. The cyclic voltammograms (CVs) are recorded at a sweep rate of 50 mV s^{-1} in N_2 or O_2-saturated electrolyte. Linear sweeping voltammograms (LSVs) are recorded in O_2-saturated electrolyte at a scan rate of 5 mV s^{-1} with different rotation speeds. For methanol tolerance and stability measurements, the chronoamperometric response curves (I-t) are acquired in O_2-saturated electrolyte at 0.6 V (rotating speed, 1600 rpm). The HER and OER results are also studied in 0.5 M H_2SO_4 and 1 M KOH solution, respectively. The following K-L equation is employed to calculate the kinetic current density (J_K) and electron transfer number (n) during the ORR.

$$J^{-1} = J_L^{-1} + J_K^{-1} = B^{-1}\,\omega^{-1/2} + J_K^{-1} \qquad (1)$$

$$B = 0.2nFC_0D_0^{2/3}\,\upsilon^{-1/6} \qquad (2)$$

$$J_K = nFkC_0 \qquad (3)$$

Where J_L and J represent the diffusion-limiting and overall current densities, ω represents the rotation speed (rpm), F represents the Faraday constant, C_0 represents the dissolved O_2 concentration, D_0 represents the O_2 diffusion coefficient, υ represents the kinematics viscosity.

Table S1. The content of C, N, O, P and Co in Co_2P/N-HCRs measured by EDX.

Sample	C (at %)	N (at %)	O (at %)	P (at %)	Co (at %)
Co_2P/N-HCR-1	79.71	1.15	8.59	3.36	7.19
Co_2P/N-HCR-2	74.65	2.10	8.32	5.06	9.87
Co_2P/N-HCR-3	68.94	2.91	9.10	6.31	12.74

Table S2. BET surface area, total pore volume and average pore size of Co_2P/N-HCRs.

Sample	BET surface area (m^2 g^{-1})	Total pore volume (cm^3 g^{-1})	Average pore size (nm)
Co_2P/N-HCR-1	186.7	0.27	7.33
Co_2P/N-HCR-2	224.1	0.29	5.87
Co_2P/N-HCR-3	141.3	0.21	4.96

Table S3. The content of C, N, O, P and Co in Co_2P/N-HCRs measured by XPS.

Sample	C (at %)	N (at %)	O (at %)	P (at %)	Co (at %)
Co_2P/N-HCR-1	86.29	0.98	7.40	1.91	3.42
Co_2P/N-HCR-2	83.01	1.94	7.76	2.54	4.75
Co_2P/N-HCR-3	79.82	2.65	8.51	3.38	5.64

Table S4. The comparison of the E_0, $E_{1/2}$ and J_i for ORR of Co_2P/N-HCRs and 20% Pt/C in O_2-saturated 0.1 M KOH at the rotation of 1600 rpm.

Sample	E_p vs RHE (V)	E_0 vs RHE (V)	$E_{1/2}$ vs RHE (V)	J_i vs RHE (V)
Co_2P/N-HCR-1	0.729	0.874	0.735	4.79
Co_2P/N-HCR-2	0.795	0.962	0.811	5.52
Co_2P/N-HCR-3	0.764	0.917	0.775	5.12
20% Pt/C	0.827	0.989	0.830	5.41

E_0: defined as the corresponding potential when ORR current density reaches 0.1 mA cm^{-2}.

J_i: defined as the corresponding current density at the potential of 0.2 V.

Table S5. Comparison of the ORR electrochemical activity in terms of E_P, E_0 and $E_{1/2}$ among the Co based related catalysts reported so far.

Catalysts	Loading (mg cm^{-2})	E_P vs RHE (V)	E_0 vs RHE (V)	$E_{1/2}$ vs RHE (V)	References
Co_2P/N-HCR-2	**0.357**	**0.795**	**0.962**	**0.811**	**This work**
Co_2FeO_4/MWCNT	0.397	0.700	0.910	0.730	[1]
CoP	—	—	0.78	0.67	[2]
Co@CoO@N-C/C	0.421	0.790	0.920	0.810	[3]
CoxP-CNTs-1000	—	0.760	0.930	0.800	[4]
Co@Co_3O_4@C-CM	0.100	0.79	0.93	0.810	[5]
Co_2P	—	—	0.90	0.790	[6]
YS-Co/N-PCMs	0.272	0.776	0.922	0.788	[7]
Co/N-HCOs	0.272	0.790	0.920	0.810	[8]
SUCo-0.1-800	—	0.780	0.945	0.793	[9]
Co/N-C-800	0.250	0.733	0.834	0.730	[10]
N-C@Co-2	0.213	0.795	0.895	0.805	[11]

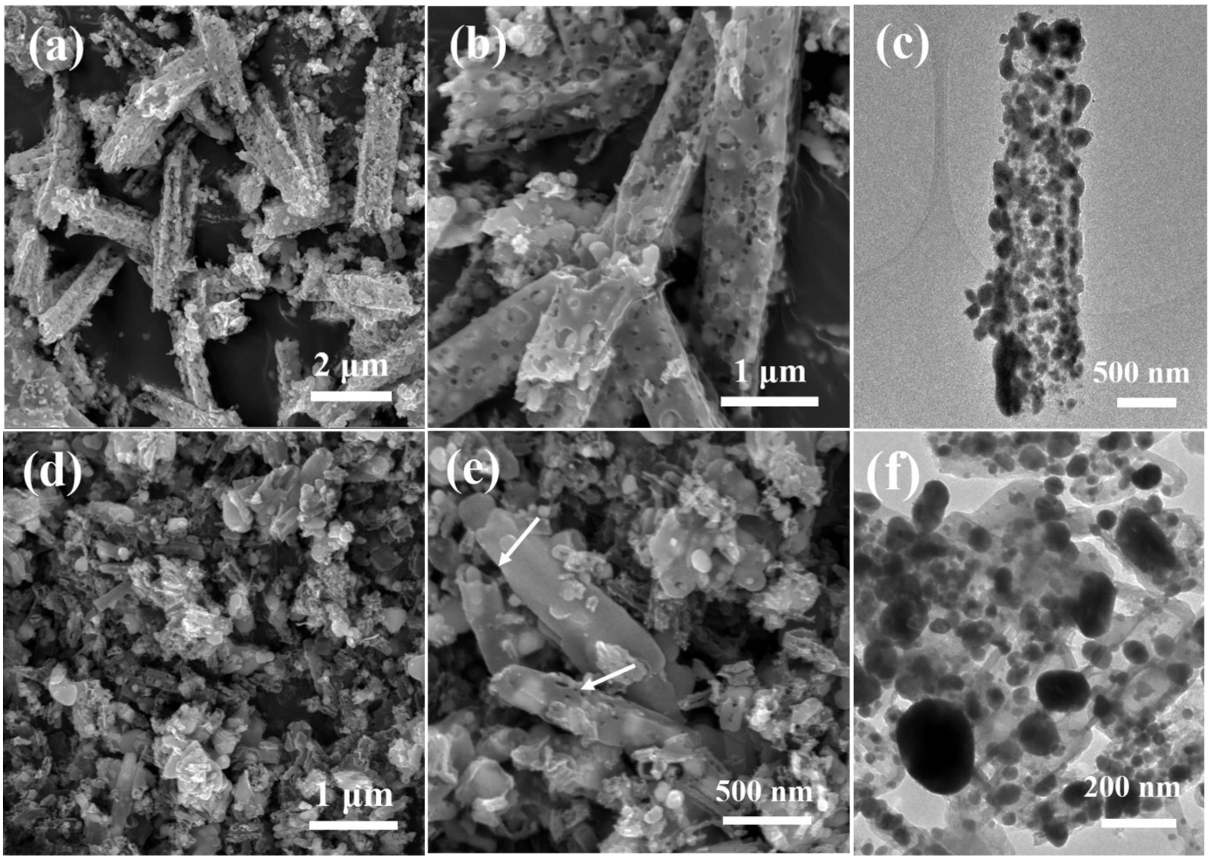

Figure S1. FESEM and TEM images of Co_2P/N-HCR-1 (a-c) and of Co_2P/N-HCR-3 (d-f).

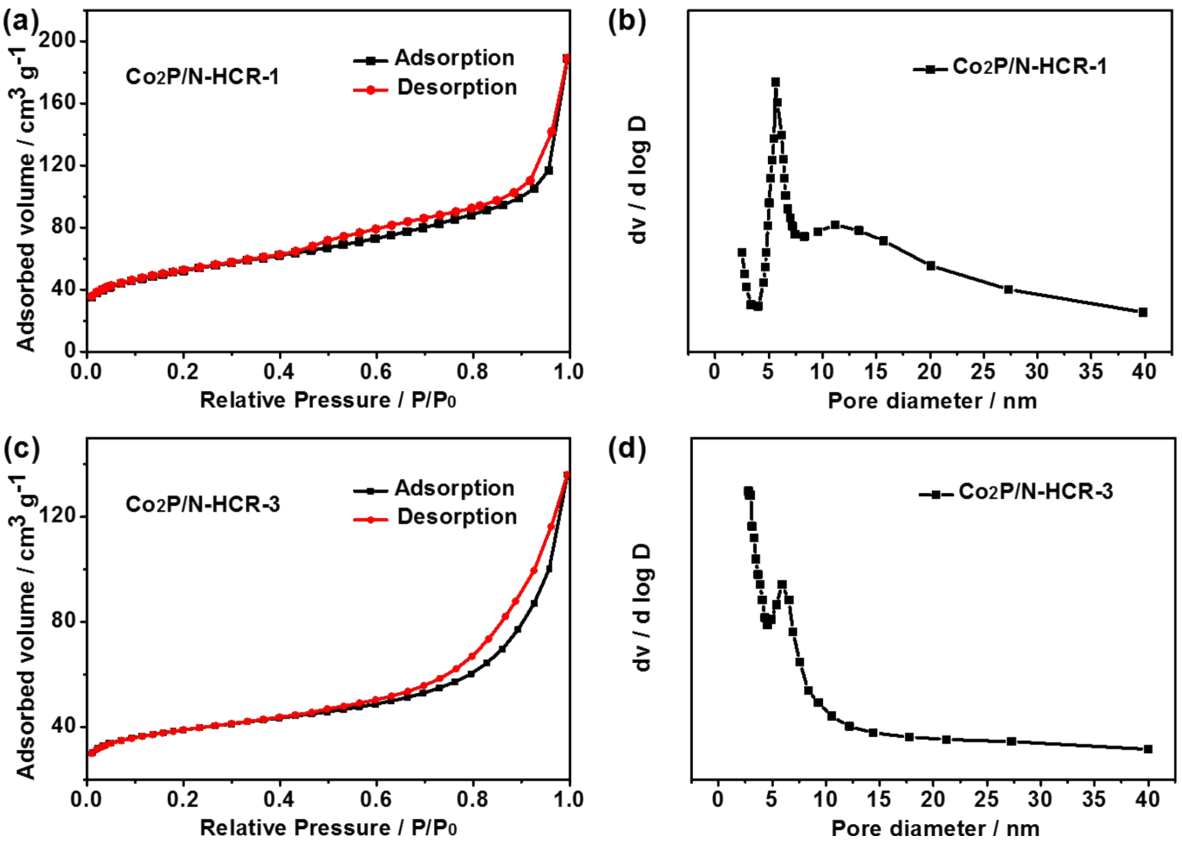

Figure S2. (a, c) Nitrogen sorption isotherms and (b, d) the corresponding pore size distribution of Co_2P/N-HCR-1 (a, b) and Co_2P/N-HCR-3 (c, d).

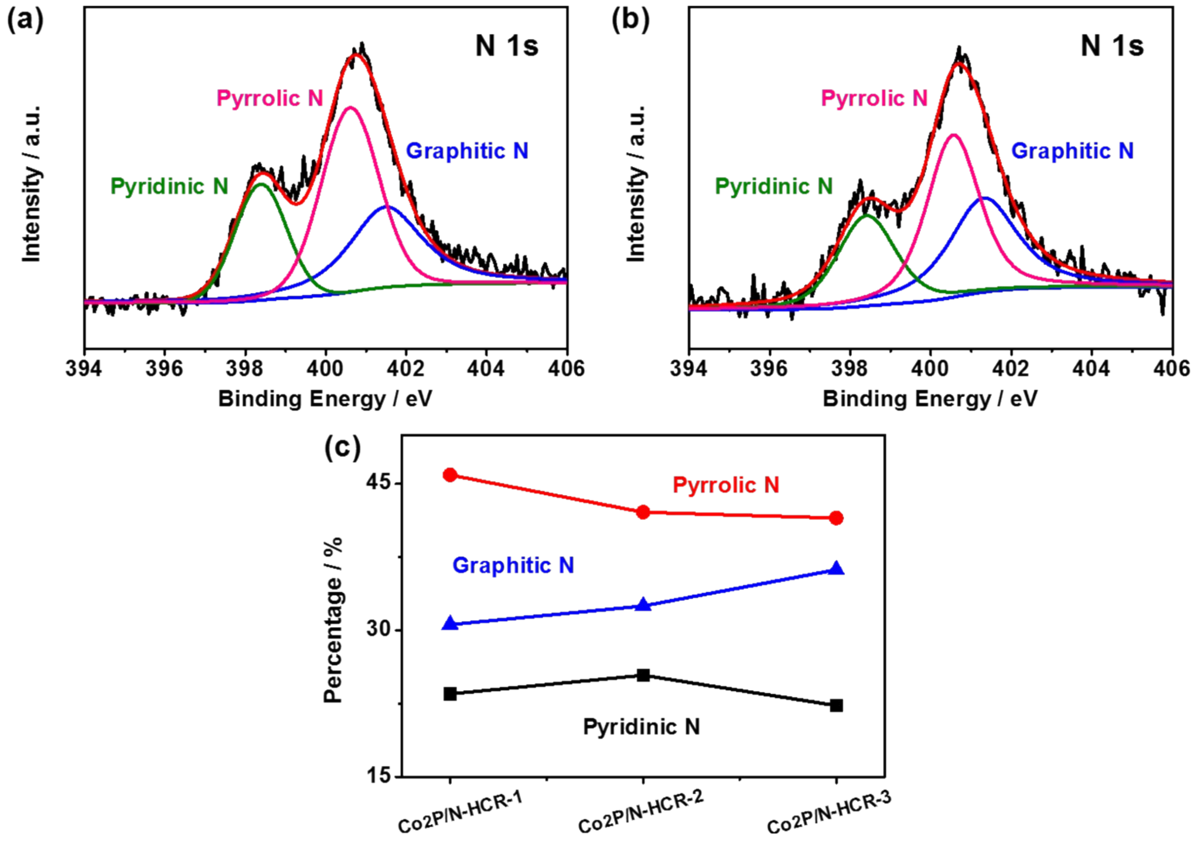

Figure S3. High-resolution N 1s spectra of Co_2P/N-HCR-1 (a) and Co_2P/N-HCR-3 (b). (c) The percentage of different N species for Co_2P/N-HCRs measured by XPS.

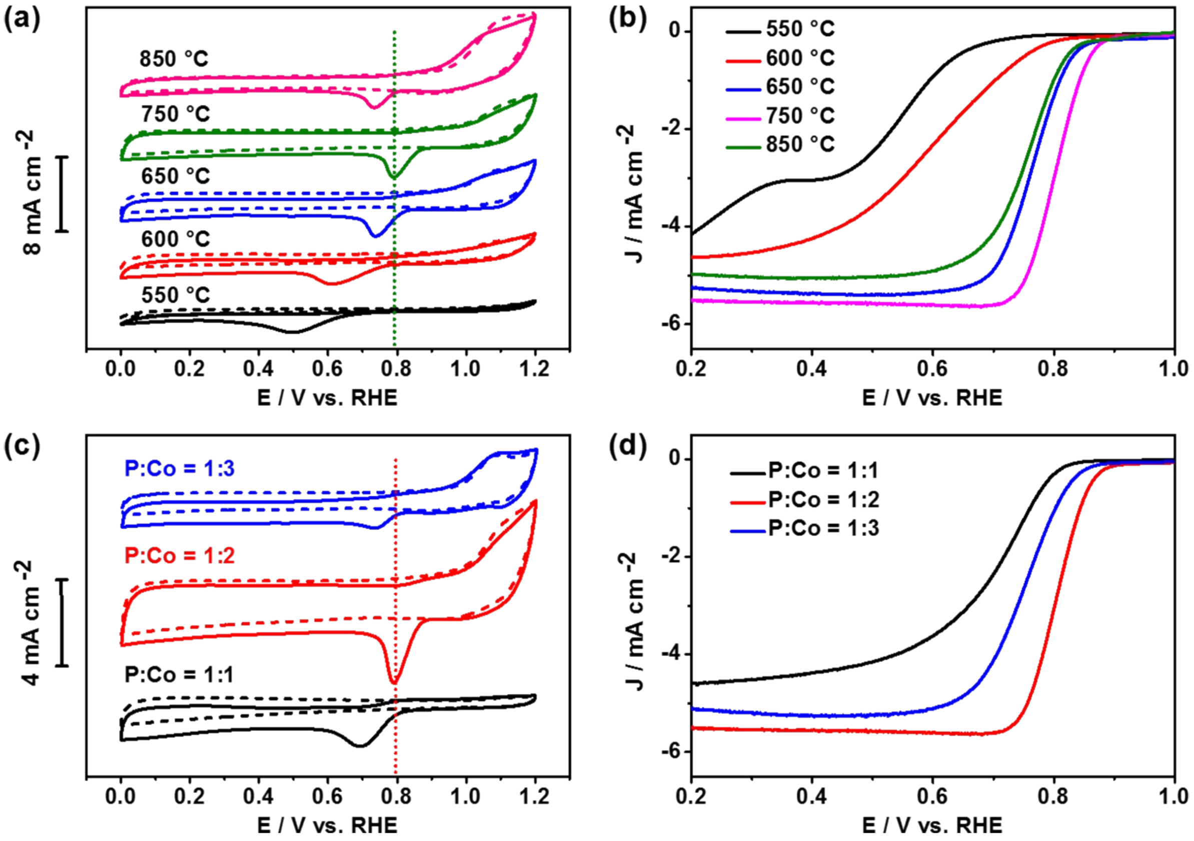

Figure S4. (a) CVs of Co_2P/N-HCR obtained at different annealing temperatures in N_2 or O_2-saturated 0.1 M KOH and (b) the corresponding LSVs in O_2-saturated 0.1 M KOH at 1600 rpm. (c) CVs of Co_2P/N-HCRs obtained at the different atomic ratios of P and Co in N_2 or O_2-saturated 0.1 M KOH and (d) the corresponding LSVs in O_2-saturated 0.1 M KOH at 1600 rpm.

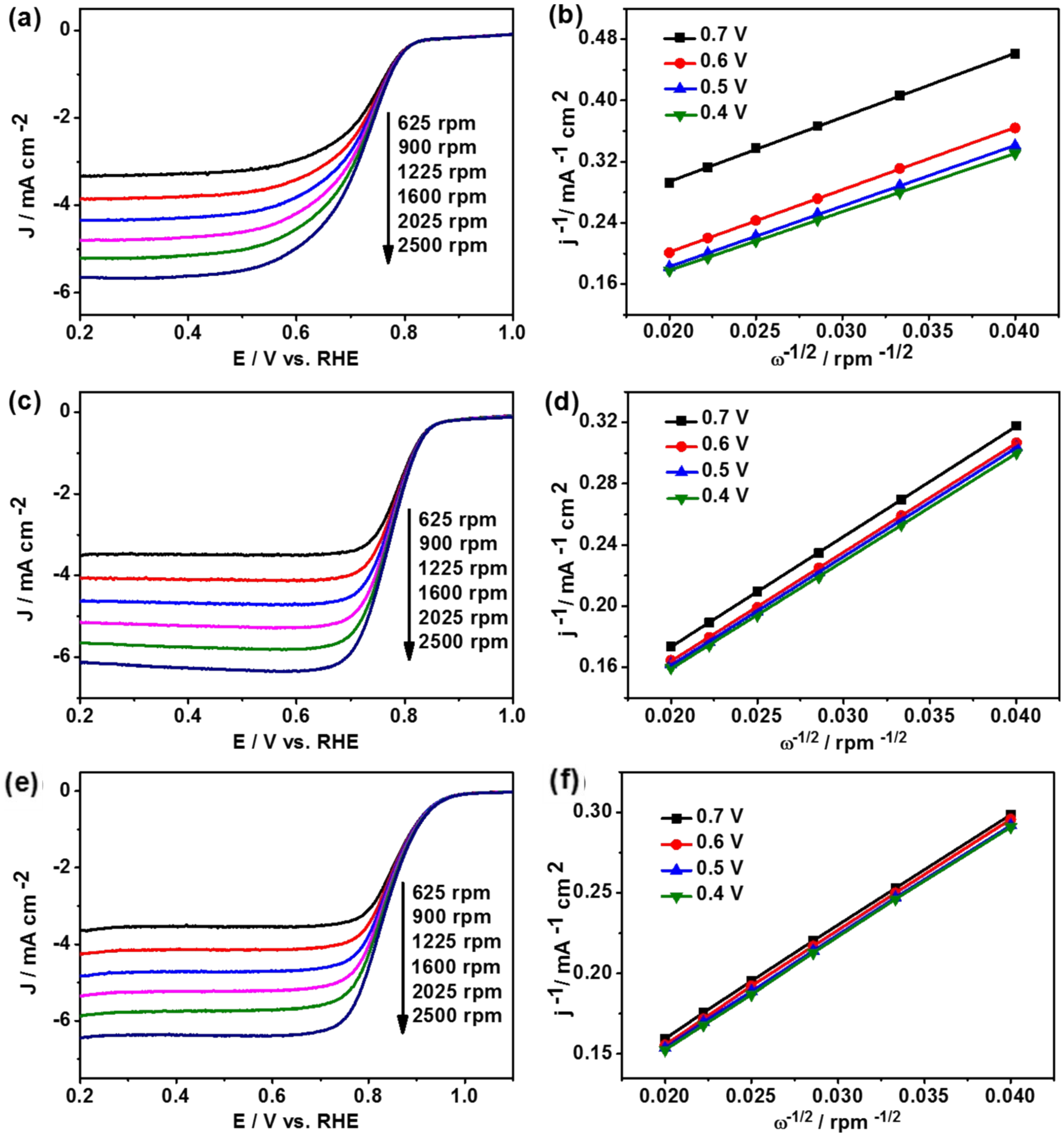

Figure S5. LSVs of Co_2P/N-HCR-1 (a), Co_2P/N-HCR-3 (c) and 20% Pt/C (e) at different rotation rates in O_2-saturated 0.1 M KOH. The corresponding K-L plots of Co_2P/N-HCR-1 (b), Co_2P/N-HCR-3 (d) and 20% Pt/C (f) at the potential range of 0.4 V to 0.7 V.

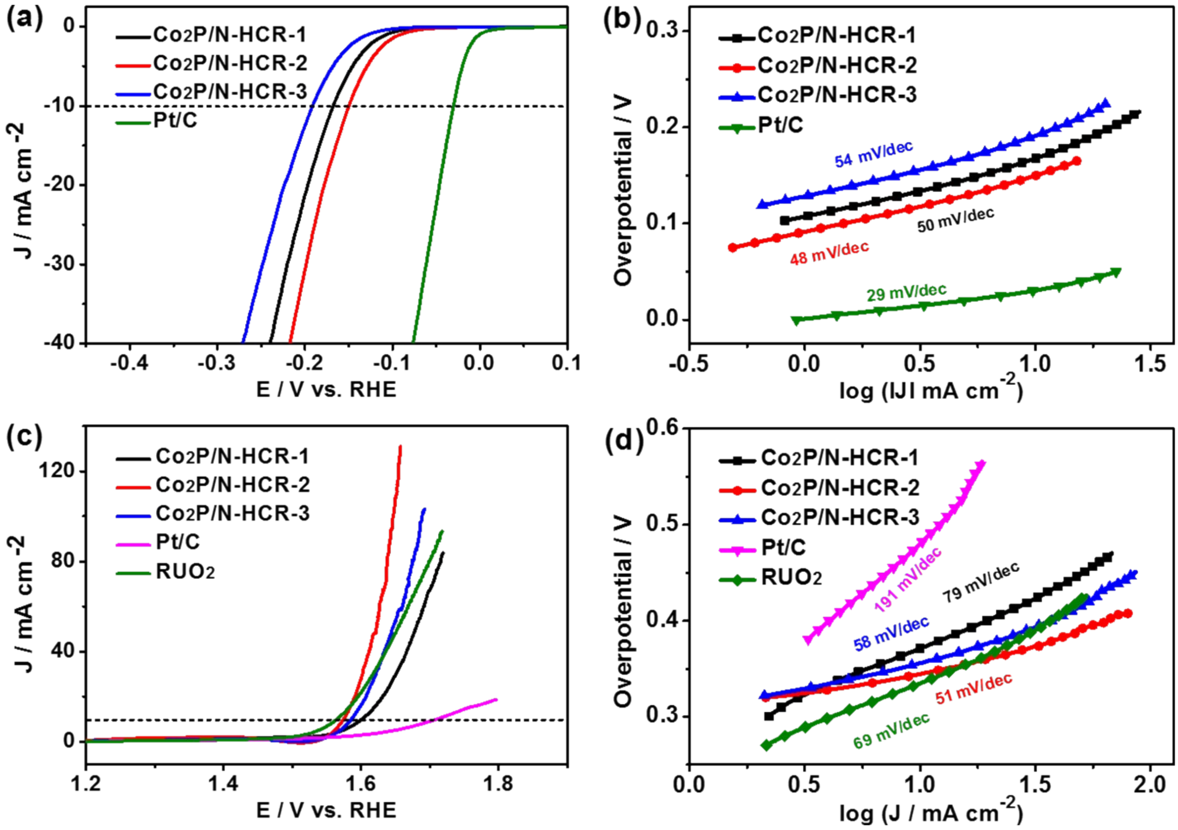

Figure S6. (a) LSVs and (b) Tafel plots of Co_2P/N-HCRs and 20 % Pt/C for HER in 0.5 M H_2SO_4. (c) LSVs and (d) Tafel plots of Co_2P/N-HCRs and 20 % Pt/C for OER in 1 M KOH.

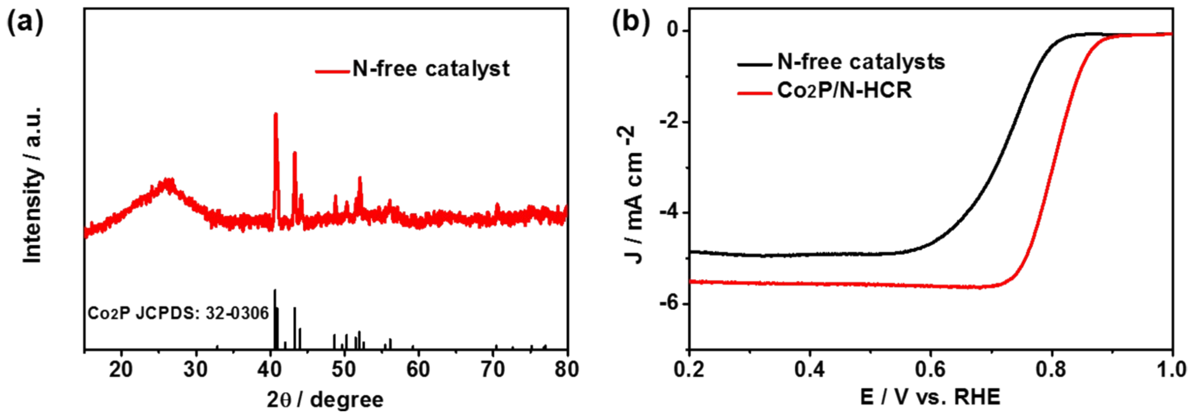

Figure S7. (a) XRD pattern and (b) LSVs of N-free catalyst and Co_2P/N-HCR in O_2-saturated 0.1 M KOH.

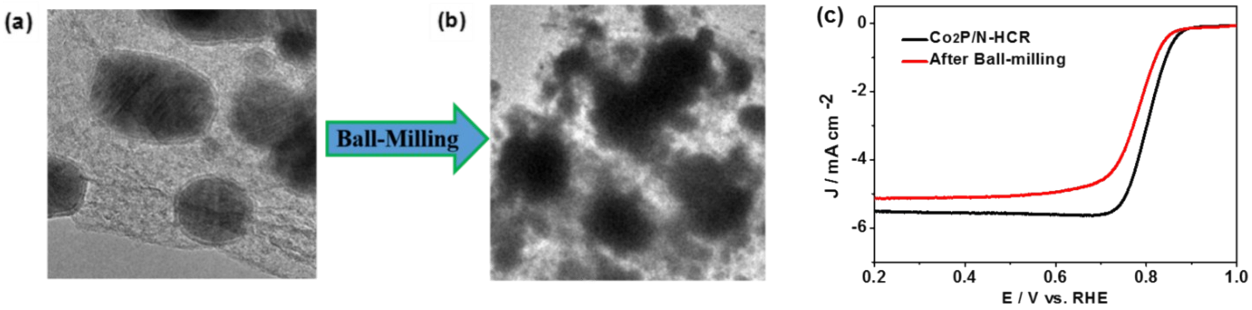

Figure S8. (a) TEM image of Co_2P/N-HCR and (b) the corresponding high-energy ball milling control catalyst. (c) LSVs of both catalysts in O_2-saturated 0.1 M KOH.

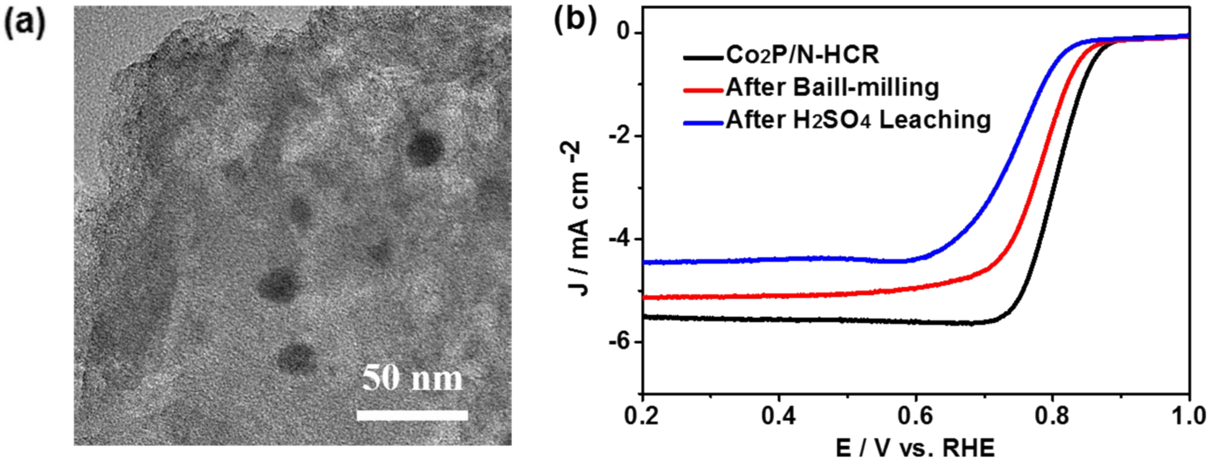

Figure S9. (a) TEM image of hot H_2SO_4 leaching control catalyst. (b) LSVs of Co_2P/N-HCR and the corresponding high-energy ball milling, hot H_2SO_4 leaching control catalysts in O_2-saturated 0.1 M KOH.

References

[1] J. Wang, H. Xin, J. Zhu, S. Liu, Z. Wu, D. Wang, J. Mater. Chem. A, 2014, **3**, 1601.

[2] H. Yang, Y. Zhang, F. Hu, Q. Wang, Nano Lett., 2015, **15**, 7616.

[3] Z. Wu, J. Wang, L. Han, R. Lin, H. Liu, H.L. Xin, D. Wang, Nanoscale, 2016, **8**, 4681.

[4] K. Chen, X. Huang, C. Wan, H. Liu, Chem. Commun., 2015, **51**, 7891.

[5] W. Xia, R. Zou, L. An, D. Xia, S. Guo, Energy Environ. Sci., 2015, **8**, 568.

[6] V.V. Doannguyen, S. Zhang, E.B. Trigg, R. Agarwal, J. Li, D. Su, K.I. Winey, C.B. Murray, ACS Nano, 2015, **9**, 8108.

[7] S. Chao, Q. Cui, K. Wang, Z. Bai, L. Yang, J. Qiao, J. Power Sources, 2015, **288**,128.

[8] S. Chao, Z. Bai, Q. Cui, H. Yan, K. Wang, L. Yang, Carbon, 2014, **82**,77.

[9] G. Zhang, W. Lu, F. Cao, Z. Xiao, X. Zheng, J. Power Sources, 2016, **302**, 114.

[10] Y. Su, Y. Zhu, H. Jiang, J. Shen, X. Yang, W. Zou, J. Chen, C. Li, Nanoscale, 2014, **6**,15080.

[11] C. Han, X. Bo, Y. Zhang, M. Li, A. Nsabimana, L. Guo, Nanoscale, 2015, **7**, 5607.